Received: 18 April 2020 | Revised: 26 June 2020 | Accepted: 6 July 2020

DOI: 10.1002/er.5811

RESEARCH ARTICLE

INTERNATIONAL JOURNAL OF ENERGY RESEARCH WILEY

A compact model for the zigzag triboelectric nanogenerator energy harvester

Akram Refaei[1] | **Mohamed Seleem**[1] | **Abdelrahman Tharwat**[1] | **Hassan Mostafa**[1,2]

[1]University of Science and Technology, Nanotechnology and Nanoelectronics Program, Giza, Egypt

[2]Electronics and Communication Engineering Department, Cairo University, Giza, Egypt

Correspondence
Hassan Mostafa, Electronics and Communication Engineering Department, Cairo University, Giza, Egypt/University of Science and Technology, Nanotechnology and Nanoelectronics Program, Giza, Egypt.
Email: hmostafa@uwaterloo.ca

Summary

Energy is a global demand nowadays. Researchers and Scientists are trying every day to find new resources to generate energy. Mechanical energy is considered one of the most essential energy resources in the world. It can be easily generated and transferred into electrical energy. There are a lot of new technologies that are working to develop small and portable energy harvesters for electronic devices such as piezoelectric and triboelectric nanogenerators (TENGs). However, TENGs are more favorable to piezoelectric nanogenerators due to the availability of nontoxic materials. Moreover, they are cheap and exhibit high performance. This article investigates one of the TENG devices, Zigzag structure. It presents an analytical derivation for the model that addresses all aspects of the TENG such as the output voltage, the output current, the capacitance, the resistive load, the capacitive load and the harvested power step by step. The analytical derivation is also verified using COMSOL simulations to validate the results. The mismatch between the analytical derivation and COMSOL is 0.022% in the open circuit voltage and 0.33% in short circuit charge. Electrical behavior is presented afterwards using Verilog-A in Cadence to examine the performance of the TENG devices in real life situations. For the chosen parameters, the device delivers a maximum voltage of 23 KV at nearly **90**° and a maximum current of 7.5 μA at nearly 10°. The maximum reported output power for a load of 5 GΩ is 5.2 mW.

KEYWORDS

analytical model, COMSOL, energy harvesting, TENG, triboelectric nanogenerators, Verilog-a, zigzag

Energy is the wheel of the modern technology and the support for its sustainability. Due to the unprecedented energy demand, scientists and researchers are continually looking for new resources to fill the gap of the insufficiency in the energy supplements.[1] Failing to submit the appropriate solutions means that the next generations will suffer from the energy insufficiency the world witnesses today. Electrical energy can be harvested from mechanical energy, chemical energy or nuclear energy. Each one of the energy sources has itsadvantages and disadvantages that make them suitable for certain situations. However, the most popular and common source is the mechanical energy since it is ubiquitous and can be easily harvested.

Mechanical Energy is considered as the most ambient source of energy in life. Waves, friction, wind and

oscillations are all examples of potential mechanical energy sources.[2] Mechanical energy is usually a renewable energy source with clean energy production and a continuous supply. However, due to the wide popularity of portable devices nowadays, new forms of mechanical energy have come into existence such as biomechanical energy sources.[3] Simply, it is the energy harvested from humans' motion such as walking, exercising and even heartbeats. It can be a direct supply for portable devices such as phones, watches and laptops.

On the other hand, a lot of limitations hinder the development of such a new technology. First of All, some of the new energy harvesters are not considered safe devices due to toxic or unstable materials included in the production processes. For instance, many piezoelectric materials are not favorable for wearable technology because of the toxic lead content.[4] Secondly, it is not a reliable technology since the energy gained is not enough to operate the devices or to continuously supply them.[5] The last important thing is that the technology encounters a lot of technological challenges on the level of the theoretical study, modeling design, fabrication and testing since it is a very emerging one.[6]

In the literature, it is encouraging to introduce two recent technologies that are investigated as energy harvesters; the piezoelectric energy harvesters and the triboelectric nanogenerators (TENGs). Piezoelectric energy harvesters have the ability to generate electric charge in response to mechanical stress. On the other hand, TENGs rely on the triboelectric effect which depends on the property of some materials to be electrically charged after they are in contact then separated from a different material. TENGs have the upper hand on the piezoelectric energy harvesters due to the high output power, high efficiency, low cost and the feasible fabrication techniques.[7]

As a result, TENGs have proved their competence from the power, efficiency and cost perspectives.[3] They are integrated in wearable technology,[8] biomedical applications and even in self-powered wireless sensors.[9] Researchers also claim that TENGs are the key towards the blue energy dream in the future.[10] TENGs have four fundamental modes: vertical contact-separation (CS) mode, lateral-sliding (LS) mode, single-electrode (SE) mode and freestanding triboelectric-layer (FT) mode. Each one of these basic modes leads to different transformed structures such as spherical, diagonal and zigzag structures. Most of the research conducted on these modes is experimental. This hinders the optimization and development of these kinds of energy harvesters. The research target is first to fully define each type with a theoretical compact form that describes the three important factors in TENG devices; the open circuit voltage (V_{OC}) and the short circuit charge (Q_{SC}) along with the distance (*V-Q-x)* relationship. The other important thing is to do modeling on the structure to save the fabrication process time and cost. However, the model should be first verified with the analytical equations to make sure that they both agree, then variations on every parameter can be conducted to test the performance. Zigzag structure has recently attracted researchers since it has a wide applications' range, good performance and relatively light weight. However, only experimental studies are performed on this structure in very slow improvements in the performance.[11] Therefore, more research is necessary to target analytical and device modeling for the Zigzag in order to accelerate the optimization and enhancement for this type of energy harvesters.

In this paper, the structure of the zigzag triboelectric nanogenerator device is presented. The analytical derivation of the zigzagis derived step by step in Section 1.1. Section 1.2 is dedicated to COMSOL simulations that verify the analytical model. The Verilog-A model has been presented in Section 1.3 to test the electrical characteristics of the device under different resistive and capacitive loads. In Section 1.4, the frequency of operation response is demonstrated. In Sections 1.5 and 1.6, the performance is investigated for different number of pairs and area variations. The conclusion summarizes the results and gives recommendations on the possible future work on the device.

1 | ZIGZAG TENG MODEL

The zigzag structure consists of two parts in which each part is divided into a dielectric and a metal layer. These two parts are connected end to end to make a series of triboelectric generators. In one design, N number of parts can be integrated to have better performance. It mainly depends on the application where this generator is implemented. The initial position is where $\theta = 0^\circ$ and the two dielectrics of each partare in contact. These dielectrics are different and have different tendency to gain or lose charges. Therefore, triboelectric charging occurs upon a separation between these two dielectrics. It is convenient to assume that a $+\sigma$ of charges is on the first dielectric and a $-\sigma$ is on the second one.[12] Upon separation and while increasing the angle between the plates, there is a charge migration from one dielectric to the other and a $V_{OC}(\theta)$ can measured between them. If an external circuit is added, it is more likely to define the electrical system by the fundamental equation of triboelectric nanogenerators[13]:

$$V(\theta) = -|Q|/C_t(\theta) + V_{OC}(\theta) \quad (1)$$

where $C_t(\theta)$ is the total capacitance of the device, $|Q|$ is the charge transferred between the two plates, $V(\theta)$ is the voltage measure at any theta at a certain load.

It treats the two plates as a capacitor and given that there are charges transferred between the two plates at a given angle, the voltage between the plates can be derived. Based on electrodynamics, both $V_{OC}(\theta)$ and $C_t(\theta)$ can be derived in order to achieve a closed form (V-Q-θ) relation.

1.1 | Analytical model

In this subsection, a detailed analytical derivation is introduced, which helps in understanding the behavior of such a mode and serves as a seed for implementing the device using circuit models.

1.1.1 | Electric Field between the two plates

The electric field between the two plates should be identified in order to use it to calculate the voltage between the plates. From electromagnetics, one can easily show for an infinite sheet of charges that the electric field is perpendicular to the surface and it is given by[14]:

$$\vec{E} = \frac{\sigma}{2\epsilon_0}\vec{n} \quad (2)$$

In Zigzag case, two electric fields each one from a plate are shown in Figure 1. The summation of them is the total electric field between the plates.

$$\vec{E}_t = \frac{\sigma}{2\epsilon_0}\vec{n_1} + \frac{\sigma}{2\epsilon_0}\vec{n_2} \quad (3)$$

A component analysis for the electric field vectors cancels out the field components in the horizontal direction since they do not cross any plates. Therefore, only components in the vertical direction are taken into account.

$$\therefore \vec{E_t} = \frac{\sigma}{2\epsilon_0}\left(\vec{n_1} + \vec{n_2}\right) = \frac{\sigma}{2\epsilon_0}\vec{a} \quad (4)$$

where

$$\vec{a} = \vec{n_1} + \vec{n_2}$$

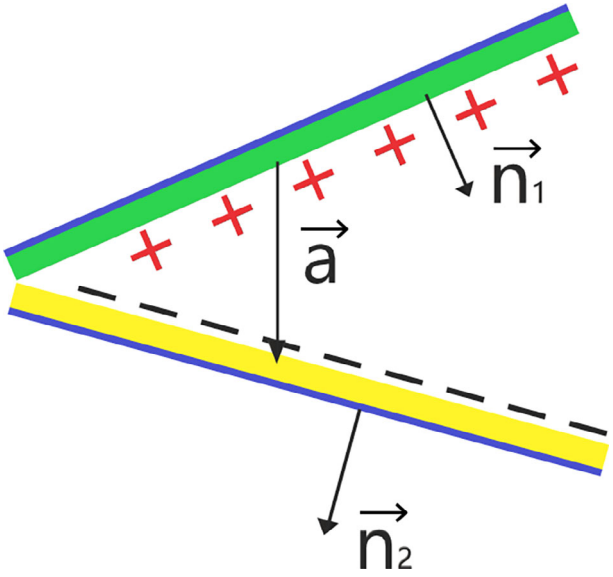

FIGURE 1 The electric field direction between the two plates [Colour figure can be viewed at wileyonlinelibrary.com]

$$\left|\vec{a}\right| = \left|\vec{n_1} + \vec{n_2}\right| = \sqrt{\left(\vec{n_1} + \vec{n_2}\right)^2} \quad (5)$$

$$\therefore \left|\vec{a}\right| = \sqrt{2}\sqrt{2\cos^2(\theta/2)} = 2\cos(\theta/2) \quad (6)$$

$$E_t = \frac{\sigma}{\epsilon_0}\cos(\theta/2) \quad (7)$$

1.1.2 | $V_{OC}(\theta)$ derivation

Each of the two plates has an area of wL. This area can be represented as a vector at the center of each plate and perpendicular to that surface. While in the electric field analysis the vertical direction is only considered, it is convenient here to do the same component analysis for the area and consider only the horizontal area (vertical area vector direction). As a result, the design can be represented instead by two parallel plates as shown in Figure 2, each with area equals: $A\cos(\theta/2)$ and a separation distance of:

$$d_{air} = 2 \cdot \frac{L}{2}\sin(\theta/2) = L\sin(\theta/2) \quad (8)$$

Since V_{oc} is defined as the voltage when no transferred charges are present ($Q = 0$) If V_{air} equals:

$$V_{air} = E_{air} \cdot d_{air} \quad (9)$$

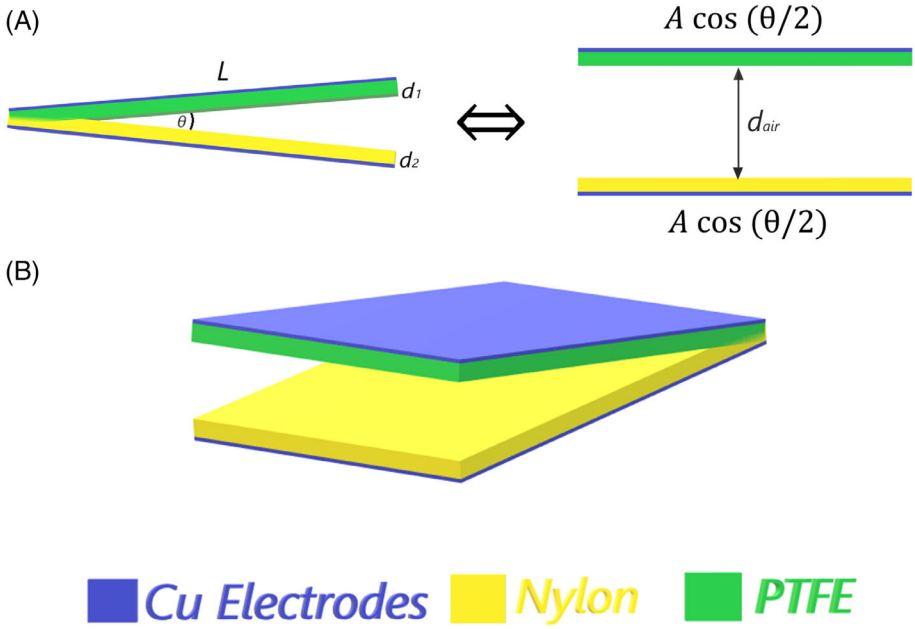

FIGURE 2 Zigzag TENG structure: (A) Equivalent zigzag and parallel plates representation (B) Device structure of the TENG model with the used materials in simulation [Colour figure can be viewed at wileyonlinelibrary.com]

And the electric field between the two plates can be written as:

$$E_{\text{air}} = \frac{-Q/A + \sigma}{\epsilon_0}\cos(\theta/2) \tag{10}$$

$$\therefore V_{\text{air}} = \frac{-Q/A + \sigma}{\epsilon_0}\cos(\theta/2)\cdot L\sin(\theta/2) \tag{11}$$

Immediately from the equations, one can show that:

$$V_{\text{OC}}(\theta) = \frac{\sigma L}{2\epsilon_0}\sin\theta \tag{12}$$

1.1.3 | $C_t(\theta)$ Derivation

To represent this structure, there are three different equivalent capacitors, one for the upper dielectric region, one for the lower dielectric region and one for the air region. Let us start with the last one:

$$\because C_{\text{air}}(\theta) = \frac{\epsilon_0 A_{\text{horizontal}}}{d_{\text{air}}} \tag{13}$$

where $C_{\text{air}}(\theta)$ is the capacitance seen between the two dielectrics as a function of theta:

$$\therefore C_{\text{air}}(\theta) = \frac{\epsilon_0 wL\cos(\theta/2)}{L\sin(\theta/2)} \tag{14}$$

It can be written also as:

$$C_{\text{air}}(\theta) = \frac{\epsilon_0 w}{\tan(\theta/2)} \tag{15}$$

The capacitance seen in the two dielectrics are $C_1(\theta)$ and $C_2(\theta)$ and their formulas can be shown in the following two equations:

$$C_1(\theta) = \frac{\epsilon_0\epsilon_{r1} wL\cos(\theta/2)}{d_1} \tag{16}$$

$$C_2(\theta) = \frac{\epsilon_0\epsilon_{r2} wL\cos(\theta/2)}{d_2} \tag{17}$$

where d_1 and d_2 are the dielectric thicknesses. ϵ_{r1} *and* ϵ_{r2} are the dielectric constants.

The device can be described as three capacitors connected in series with capacitances equal to $C_{\text{air}}(\theta)$, $C_1(\theta)$ and $C_2(\theta)$. The total capacitance of the Zigzag TENG device is given by:

$$\because \frac{1}{C_t} = \frac{1}{C_1(\theta)} + \frac{1}{C_2(\theta)} + \frac{1}{C_{\text{air}}(\theta)} \tag{18}$$

$$\therefore \frac{1}{C_t} = \frac{d_{01} + d_{02}}{\epsilon_0 wL\cos(\theta/2)} + \frac{\tan(\theta/2)}{\epsilon_0 w} \tag{19}$$

where: $d_{01} = \frac{d_1}{\epsilon_{r1}}$ and $d_{02} = \frac{d_2}{\epsilon_{r2}}$

$$\therefore C_t = \frac{\epsilon_0 wL\cos(\theta/2)}{d_{01} + d_{02} + L\sin(\theta/2)} \tag{20}$$

1.1.4 | $Q_{SC}(\theta)$ derivation

The short circuit condition requires that $V = 0$; Substituting with this condition in the TENG general equation gives:

$$Q_{SC} = V_{OC} \cdot C_t \tag{21}$$

$$\therefore Q_{SC} = \frac{\sigma L}{2\epsilon_0}\sin\theta \cdot \frac{\epsilon_0 wL\cos(\theta/2)}{d_{01} + d_{02} + L\sin(\theta/2)} \tag{22}$$

$$Q_{SC} = \frac{\sigma wL^2 \sin\theta\cos(\theta/2)}{2[d_{01} + d_{02} + L\sin(\theta/2)]} \tag{23}$$

by substituting with Q_{SC} and V_{OC} in TENG general equation one can show that:

$$V(\theta) = \frac{-|Q|}{\frac{\epsilon_0 wL\cos(\theta/2)}{d_{01} + d_{02} + L\sin(\theta/2)}} + \frac{\sigma L}{2\epsilon_0}\sin\theta \tag{24}$$

$$V(\theta) = \frac{-|Q|(d_{01} + d_{02} + L\sin(\theta/2))}{\epsilon_0 wL\cos(\theta/2)} + \frac{\sigma L}{2\epsilon_0}\sin\theta \tag{25}$$

However, in most cases, Q_{SC} term is not useful sinceonly the current can be measured. Consequently, it is more appropriate to derive a formula for I_{SC}:

$$\because I_{SC} = \frac{dQ_{SC}}{dt} \tag{26}$$

$$\therefore I_{SC} = \frac{\sigma wL^2}{2} \cdot \frac{d}{dt}\left\{\frac{A}{B}\right\} = \sigma wL^2 \cdot \frac{dA \cdot B - A \cdot dB}{B^2} \tag{27}$$

where $A = \sin\theta\cos(\theta/2)$

$$B = z + L\sin(\theta/2)$$

$$z = d_{01} + d_{02} = \frac{d_1}{\epsilon_{r1}} + \frac{d_2}{\epsilon_{r2}}$$

$$\therefore I_{SC} = \sigma wL^2 \cdot \omega \cdot \frac{\left[\cos\theta \cdot \cos\left(\frac{\theta}{2}\right) - \frac{1}{2}\cdot\sin\theta 1 \cdot \sin\left(\frac{\theta}{2}\right)\right] \cdot \left[z + L\sin\left(\frac{\theta}{2}\right)\right] - \frac{1}{2}L\sin\theta\cos^2\left(\frac{\theta}{2}\right)}{2\left[z + L\sin\left(\frac{\theta}{2}\right)\right]^2}$$

$$\text{and } \omega = \frac{d\theta}{dt} \tag{28}$$

As one can notice, the current is a function of speed of motion of the plates, the faster the plates, the more current is generated.

1.2 | COMSOL simulations

COMSOL-MULTY-PHYSICS 5.3 is used as a finite element method tool to simulate the design. All used design parameters are listed in Table I, the parameters selection for the device is mainly dependent on the target application. The surface charge density is based on materials' experimental data presented in Reference 15 to have high output voltage. The structure is surrounded by air to model the real-lifesituations. Moreover, the maximum angle is chosen from the literature for practical purposes.[16] The results of the simulations are shown in Figure 3(a) and (b) with calculated average errors between the analytical derivations and the simulations for $V_{OC}(\theta)$ and $Q_{SC}(\theta)$.

1.3 | Zigzag Verilog-A model

A TENG structure is modeled by a lumped parameter equivalent circuit model as an ideal arbitrarily time-varying voltage source $V_{OC}(\theta(t))$ serially connected to a capacitor $C(\theta(t))$ as shown in Figure 4.[17]

1.3.1 | Resistive load

Considering the case of a pure resistive load, the (V-Q-θ) relationship can be expressed as follows:

$$V(\theta) = \frac{-|Q|}{\frac{\epsilon_0 wL\cos(\theta/2)}{d_{01} + d_{02} + L\sin(\theta/2)}} + \frac{\sigma L}{2\epsilon_0}\sin\theta = R\frac{dQ(\theta)}{dt} \tag{29}$$

where R is the equivalent resistance as seen at the TENGTerminals. The power is expressed as:

$$P = V(\theta) \cdot I(\theta) = V^2(\theta)/R \tag{30}$$

From where the maximum power is:

$$P_{max} = V_{max} \cdot I_{max} \tag{31}$$

TABLE I Parameter set used in COMSOL simulation

Parameter	Value
Plate length L	4 cm
Plate width w	4 cm
Thickness of the dielectrics d_1, d_2	125 μm
Relative dielectric constants ϵ_{r1}, ϵ_{r2}	2.1, 4
Surface charge density σ	10 μC/m^2

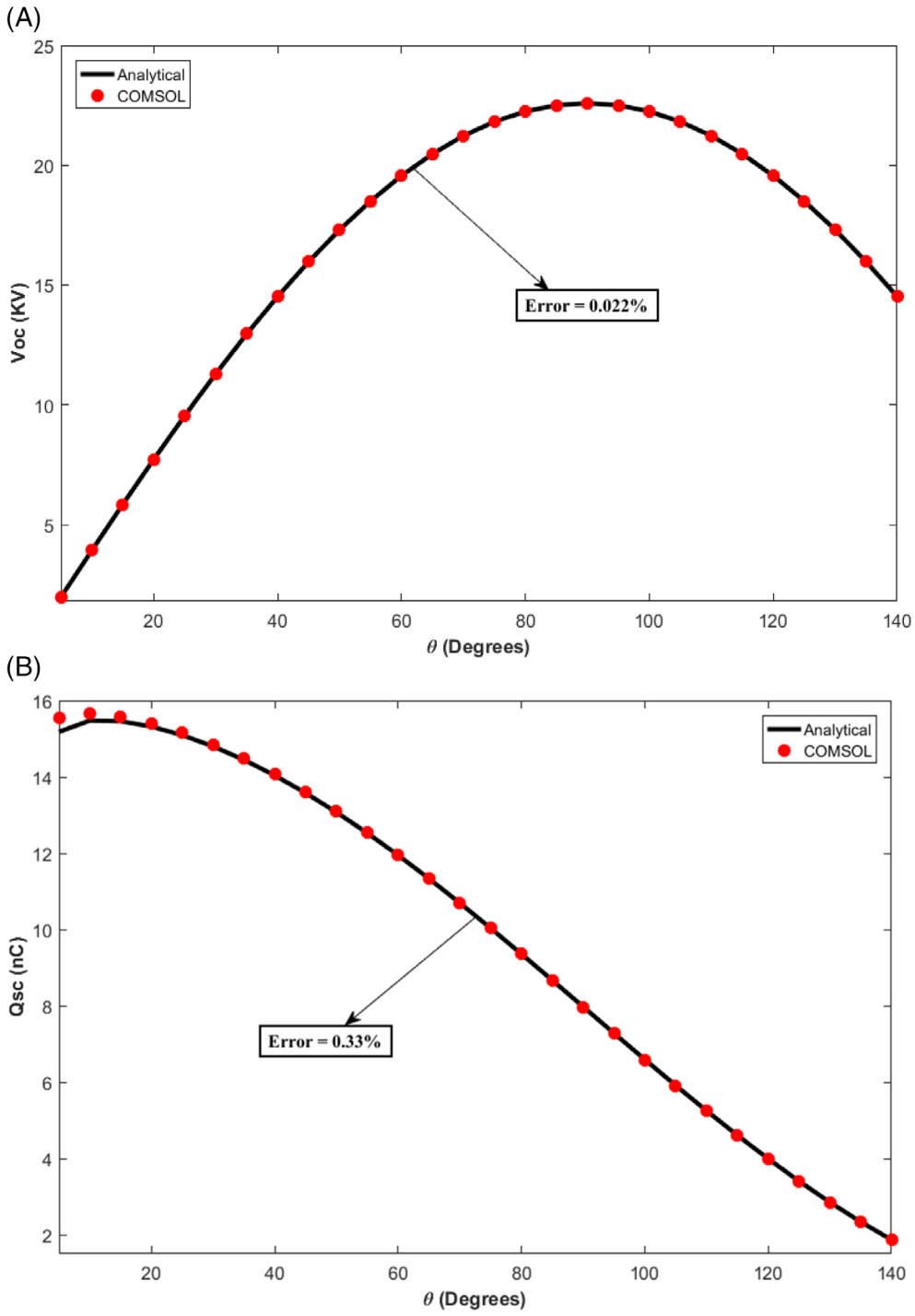

FIGURE 3 COMSOL simulation results along with the analytical derivation: (a) Open circuit voltage vs angle (b) short circuit charges vs angle [Colour figure can be viewed at wileyonlinelibrary.com]

Therefore, various circuit simulation tools (i.e., Cadence Virtuoso) can be used to study the behavior of device under different load resistance.

A study for the voltage under different load Resistance is present in Figure 5. In the case of open circuit condition ($R = \infty$), the output voltage increases rapidly and has a maximum value $\approx$ 23 KV exactly as expected by the analytical equations and COMSOL simulations, when the load decreases, the maximum voltage decreases until it becomes zero. For relatively high loads, the maximum voltage occurs at $\approx 90^{\circ}$. This can be expected easily from the equations ($V \propto R$). When no load present between the two terminals, the voltage is zero as expected which is the case of short circuit condition.

The transferred charges between the two plates also are graphed in Figure 6. At the short circuit condition ($R = 0$), the charge graph is identical to the analytical and the simulation. It is expected that the current would be constant at most of the range since the charges exhibit linear behavior. Otherwise, the

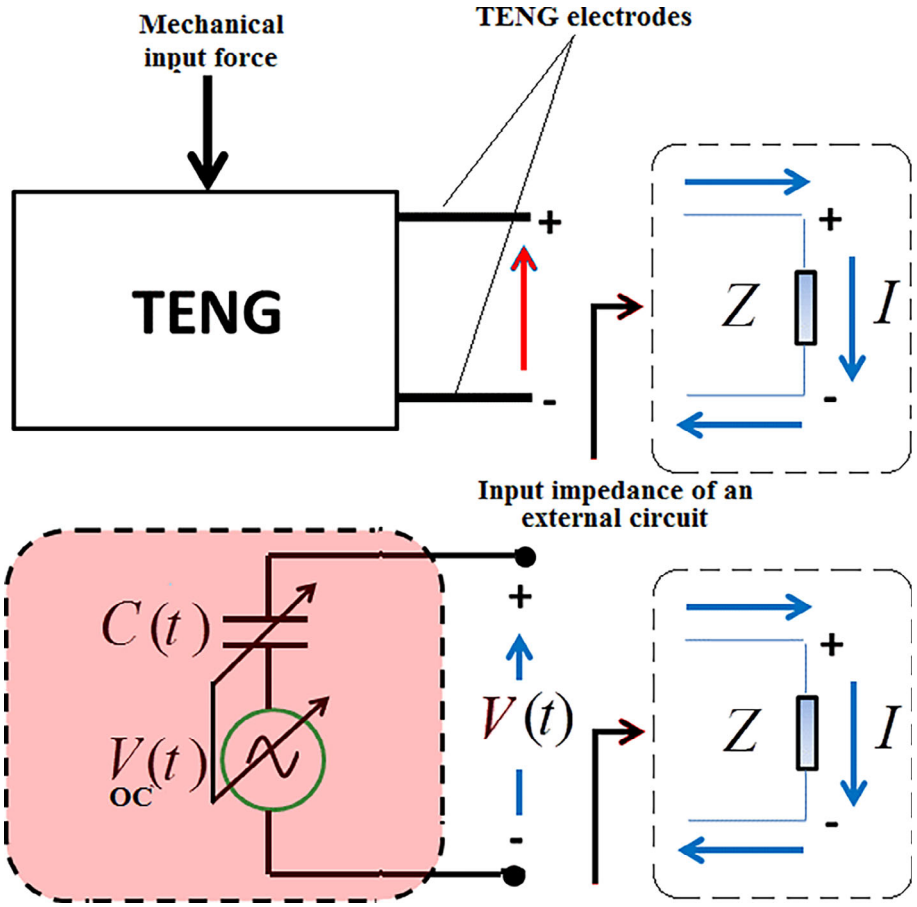

FIGURE 4 Schematic representation of the Zigzag equivalence circuit with an arbitrary load[17] [Colour figure can be viewed at wileyonlinelibrary.com]

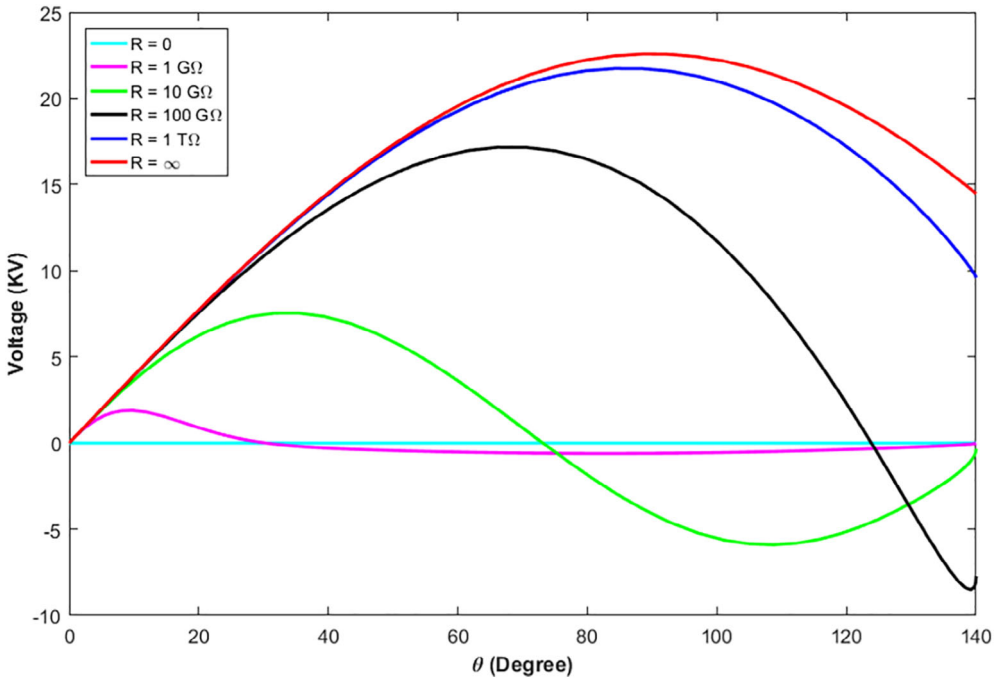

FIGURE 5 Output voltage versus the angle of motion for different load resistance [Colour figure can be viewed at wileyonlinelibrary.com]

current would be varying with the angle and an external platform needs to be integrated to have a DC behavior.

Figure 7, at the short circuit condition ($R = 0$), the current has a maximum value nearly at $I = 7.5$ μA. However, once a load is applied to the device, the current

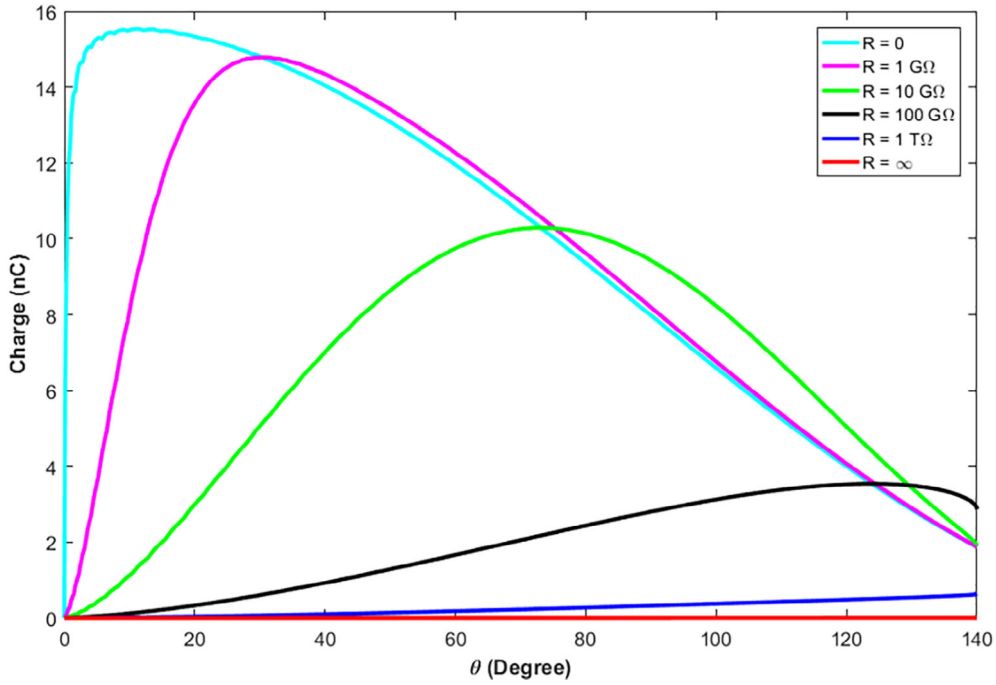

FIGURE 6 The transferred charge between the plates vs the angle of rotation under different resistive loads [Colour figure can be viewed at wileyonlinelibrary.com]

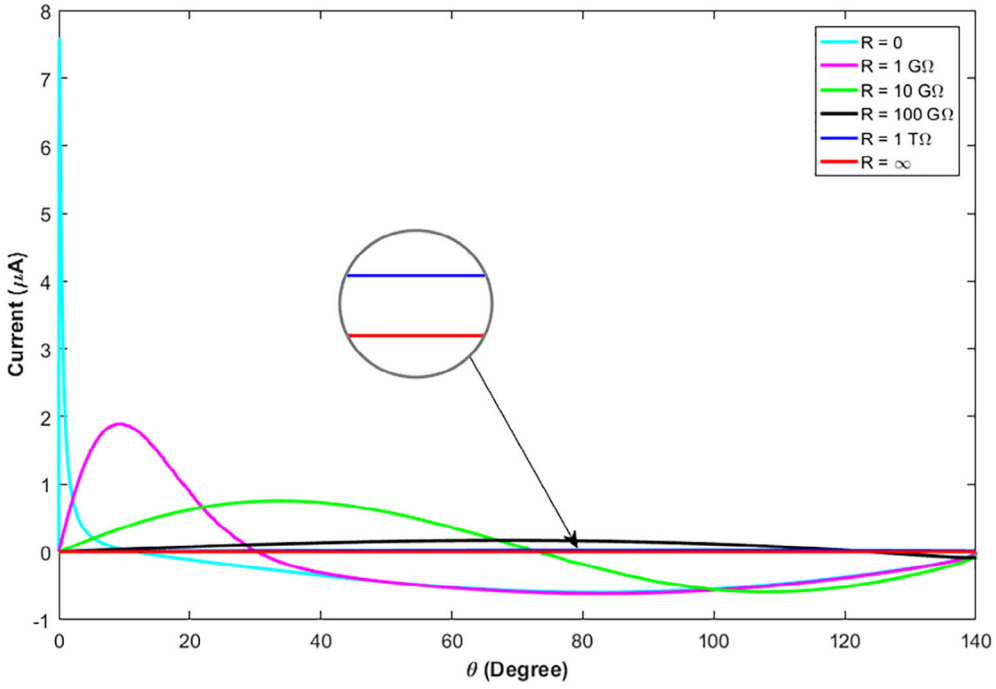

FIGURE 7 Output current versus the angle of motion for different load resistance [Colour figure can be viewed at wileyonlinelibrary.com]

degrades while increasing the load resistance until it reaches zero. The maximum current while a load is connected occurs at ($\theta = 10^{\circ}$) with a load resistance of 1 GΩ; Therefore, it is preferable for systems that need a start with a high peak current to adjust the load to be at this range.

The maximum current and voltage under different load resistance are indicated in Figure 8. It shows that the optimal performance point is at $\approx 5 \times 10^9$ Ω that corresponds to a maximum voltage of ≈ 4 KV and a maximum current of ≈ 1.3 μA. This gives power of 5.2 mW.

Figure 9 shows the maximum power retrieved from the zigzag device over the load resistance. It is recommended to keep the resistance around 5×10^9 Ω to get a maximum power of ≈ 5.2 mW.

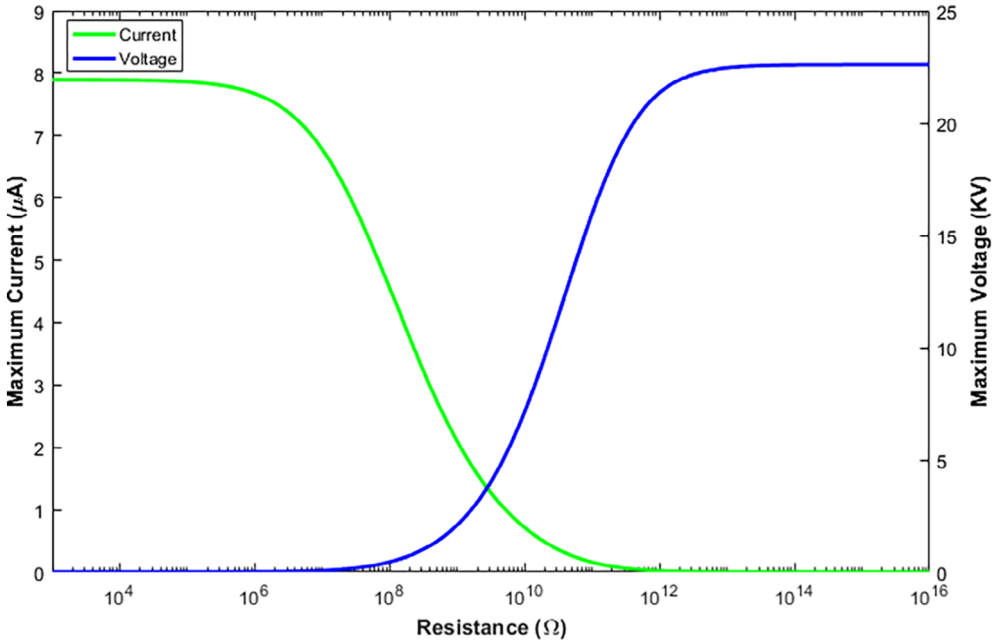

FIGURE 8 Maximum voltage and maximum current versus the load Resistance showing the best optimal load point [Colour figure can be viewed at wileyonlinelibrary.com]

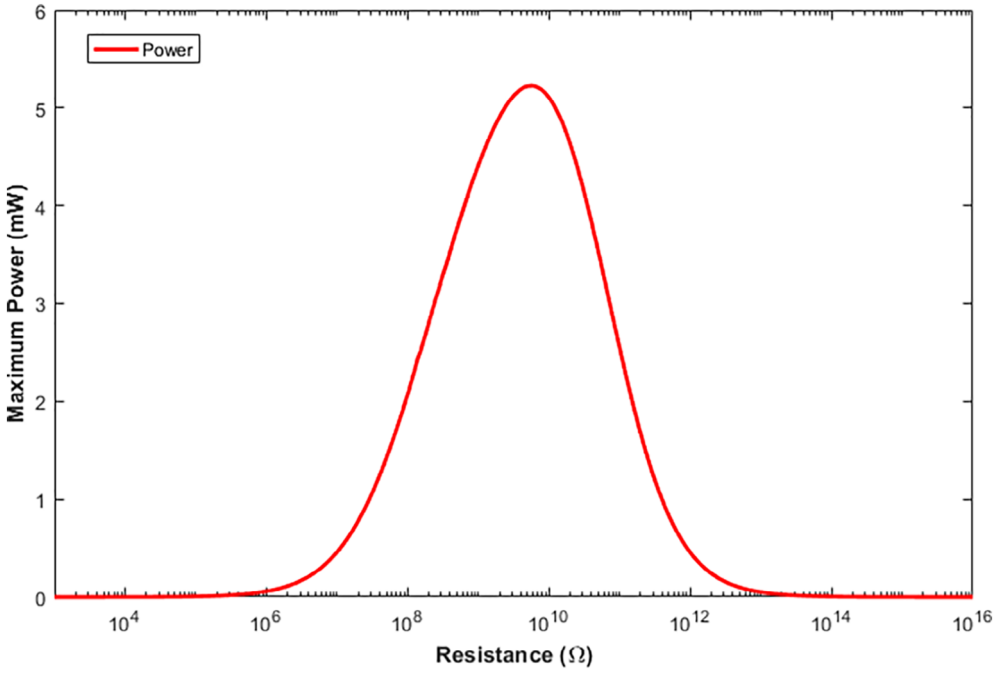

FIGURE 9 The maximum power over the load resistance [Colour figure can be viewed at wileyonlinelibrary.com]

1.3.2 | Capacitive load

The energy harvesters are usually connected to energy storage elements such as capacitors. Capacitors are stabilizing the output of the energy harvesters since minor changes in the surrounding may lead to unstable output.[18] The same analysis is performed on a load capacitance. Given that the TENG fundamental equation is:

$$V(\theta) = -|Q|/C_t(\theta) + V_{OC}(\theta) = Q/C_L \tag{32}$$

$$\therefore Q_C = C_L V(\theta) \tag{33}$$

where Q_C is the charge on the capacitor.

According to,[19] the capacitive load equations are derived using the initial conditions at $t = 0$, the zigzag plates are in contact initially and the angle is zero.

$$Q_c - Q = Q_c(t=0) - Q(t=0) = 0 \tag{34}$$

$$\therefore Q = Q_C = C_L V \tag{35}$$

Given that the energy stored in the capacitor equals:

$$E_c = \frac{1}{2} C_L V^2 \tag{36}$$

$$V = -\frac{C_L V}{C_t} + V_{OC} \tag{37}$$

$$\therefore V = \frac{C_t V_{OC}}{C_t + C_L} = \frac{Q_{SC}}{C_t + C_L} \tag{38}$$

$$E_C = \frac{1}{2} C_L V^2 = \frac{C_L Q_{SC}^2}{2(C_t + C_L)^2} \tag{39}$$

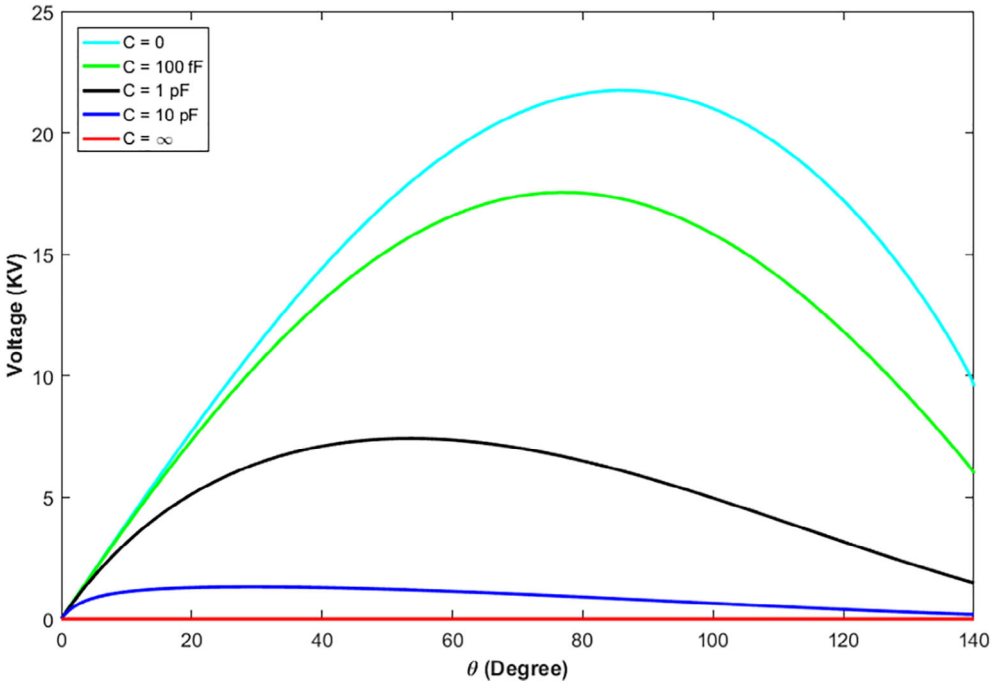

FIGURE 10 Output voltage versus the angle of motion for different load capacitance [Colour figure can be viewed at wileyonlinelibrary.com]

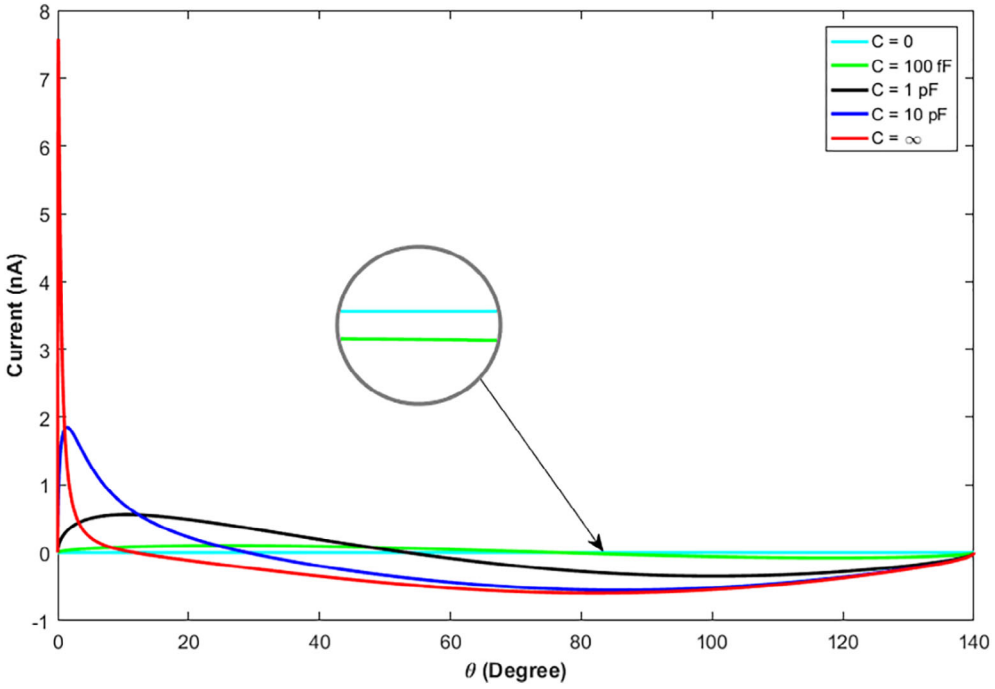

FIGURE 11 Output current versus the angle of motion for different load capacitance [Colour figure can be viewed at wileyonlinelibrary.com]

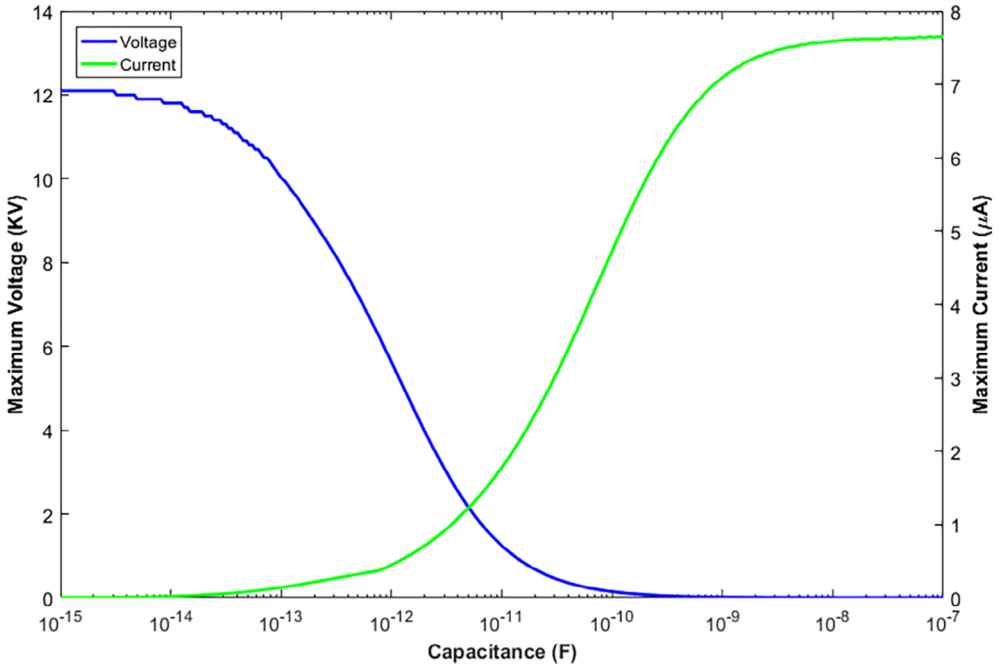

FIGURE 12 Voltage and maximum current versus the load capacitance showing the best optimal load point [Colour figure can be viewed at wileyonlinelibrary.com]

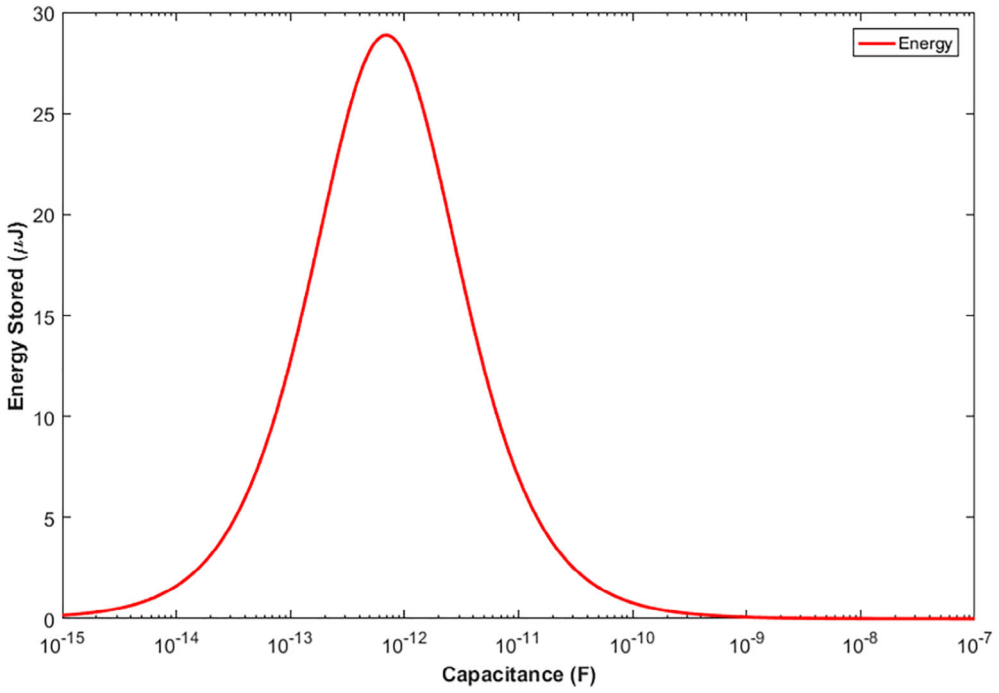

FIGURE 13 The energy stored over the load capacitance [Colour figure can be viewed at wileyonlinelibrary.com]

Using a very valid approximation where:

$$L \gg z$$

The stored energy is expressed as:

$$E_c = \frac{\sigma^2 w^2 L^2 \sin^2(\theta)}{8C_L\left[\tan\left(\frac{\theta}{2}\right) + \frac{\epsilon_0 w}{C_L}\right]^2} \tag{40}$$

The same analysis is done for capacitive load instead of resistive one. In Figure 10, for relatively large capacitive load, the voltage is ≈ zero. However, for small loads, unlike the resistive load, it is noticed that the voltage rises while increasing the angle until nearly 90° then drops. It is worth to mention that $V \approx 23$ KV for no load capacitance and $V \approx 18$ KV for $C_L = 100$ fF.

The current exhibits opposite behavior under the same load as expected as in Figure 11. There is no current

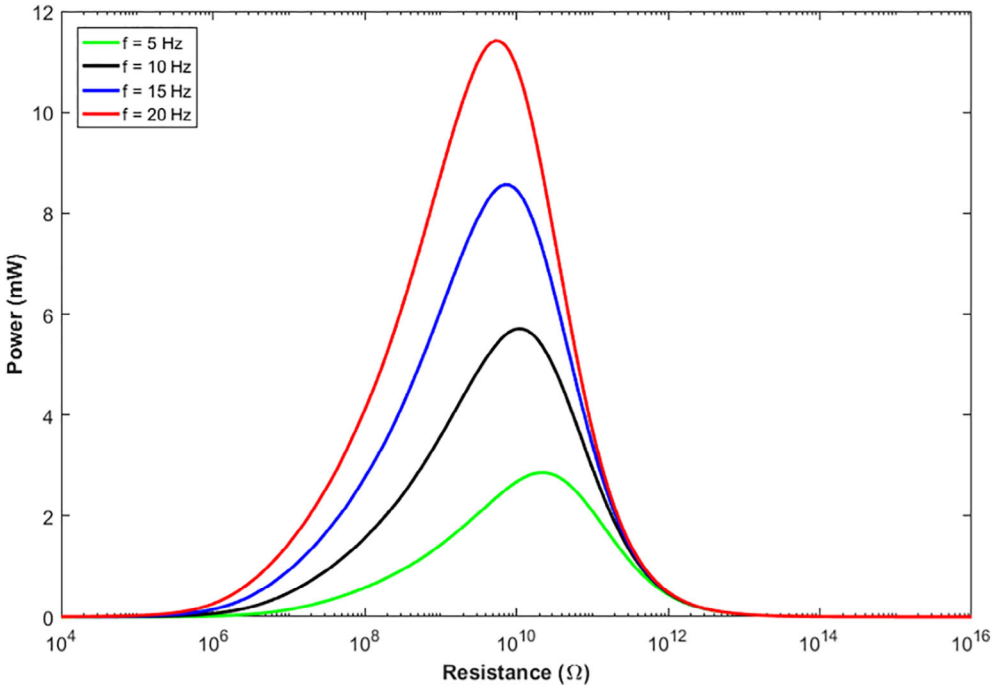

FIGURE 14 The maximum power versus the load resistance for different frequencies [Colour figure can be viewed at wileyonlinelibrary.com]

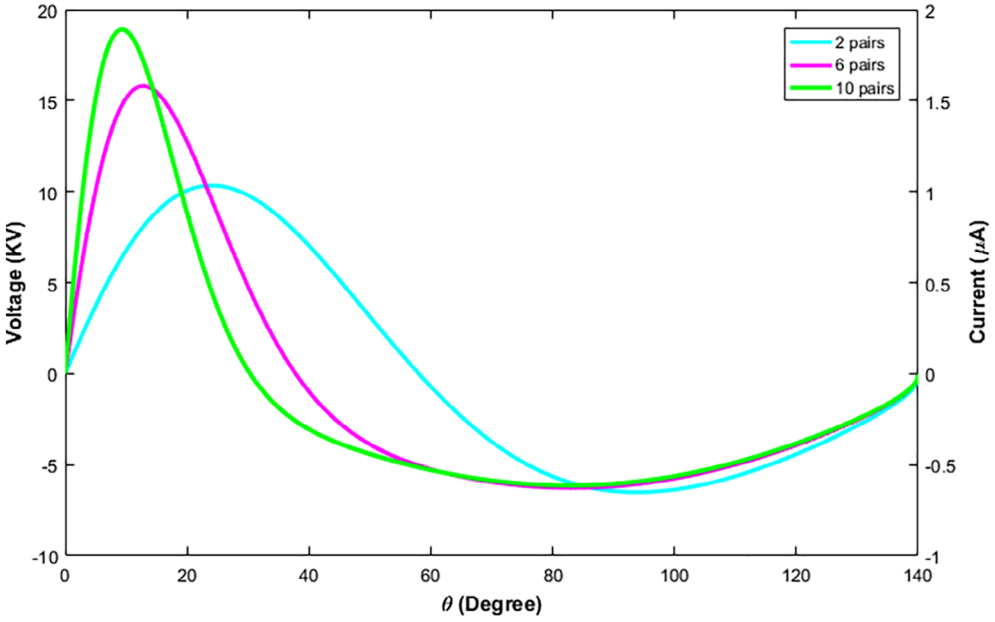

FIGURE 15 Output voltage and output current versus the angle of motion for different number of pairs [Colour figure can be viewed at wileyonlinelibrary.com]

for ≈ *zero* load capacitance. The current has a maximum value very early at ≈ 3° for a very high capacitance. This maximum point shifts to higher degrees while lowering the capacitance value and correspondingly the current decrease.

Although these two curves have illustrated some aspects of the Zigzag behavior under different loads, they do not give an insight for the range of the capacitance at which the maximum current and the maximum voltage can be determined. Therefore, a plot of the maximum voltage and the maximum current is obtained to determine the best load. Figure 12 shows that for a load capacitance of $\approx 8 \times 10^{-12}$ F, an optimal performance is present for the maximum voltage and maximum current at the same time. The reported values are ≈ 2 KV and ≈ 1.8 μA for the voltage and the current respectively. This gives power of 3.6 mW.

A study for the Energy Storedfor the zigzag device under the load capacitance is important since some applications depend on the maximum energy stored in the system. Figure 13, at nearly 10^{-12} F, there is a peak for the energy stored with ≈ 28 μJ. As a result, the load must be

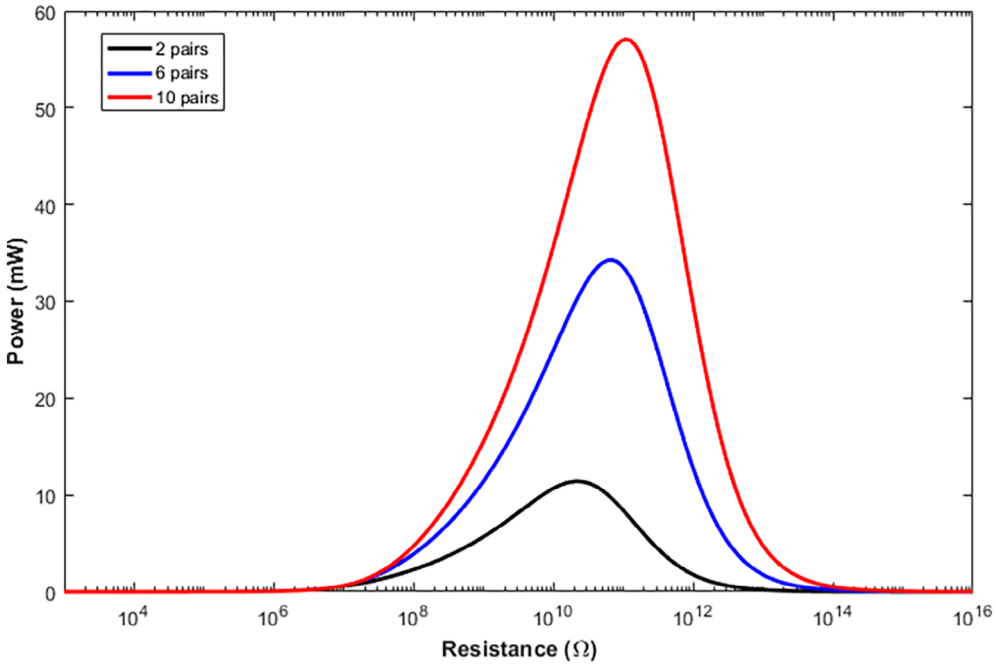

FIGURE 16 The maximum power versus the load resistance for different number of pairs [Colour figure can be viewed at wileyonlinelibrary.com]

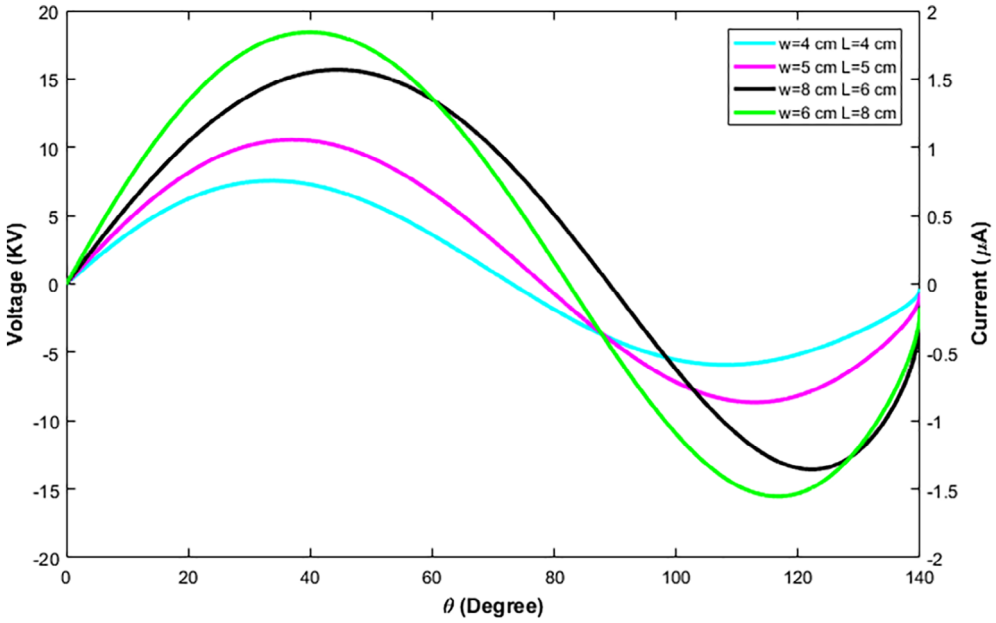

FIGURE 17 Output voltage and output current versus the angle of motion for different physical dimensions [Colour figure can be viewed at wileyonlinelibrary.com]

around this value according to the maximum power transfer theory proven in (40).

1.4 | Performance under different frequency conditions

It is important to study the frequency response of the device to determine the best angular velocity of motion for this device. Moreover, the range of the resistive load that can be applied is identified from the power curve. In Figure 14, at a resistive load of $\approx 10^{10}\Omega$, optimal power performance is obtained for 5, 10, 15 and 20 Hz frequencies with 3, 5, 8.5 and 11.5 mW optimal power respectively. A right shift is observed in the power curve while the frequency decreases. This is suitable for low power high impedance applications.

1.5 | Performance under different number of pairs

Since Zigzag device is usually used in a series connection, it is crucial to investigate the voltage, current and

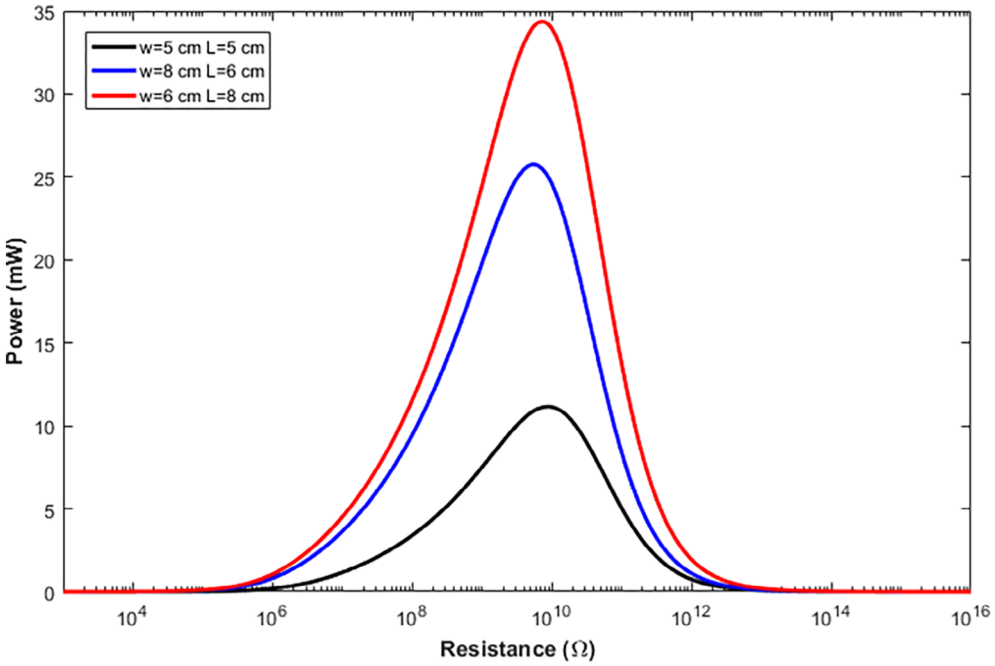

FIGURE 18 The maximum power vs the load resistance for different physical dimension [Colour figure can be viewed at wileyonlinelibrary.com]

power of the device under different number of pairs. Figure 15 shows the behavior of the Zigzag for two, six and ten pairs for a load resistance of 10 GΩ. As the number of pairs is increased, the voltage and the current are increasing also.

Figure 16 shows the power of the Zigzag device under different load resistance. The peak shifts to the right while increasing the number of pairs. The optimal power values are 12, 35 and 58 mW corresponding to 20, 90 and 200 GΩ.

1.6 | Performance under area variations

This section is dedicated to study the output characteristics while changing the physical dimensions of the device. The device is assumed to be a rectangle pair. For a resistive load of 10 GΩ, a comparison is demonstrated against the used physical parameters above. Figure 17 shows the voltage and current outputs under different dimensions of the Zigzag. While increasing the area, they exhibit higher magnitude value. However, for the last two curves with the same area of 48 cm^2, (29) explains that the voltage is a strong function of the length of the Zigzag but not the Width. Therefore, increasing the device length is much more important than increasing the width.

To obtain the best matching resistive load, the output power is shown vs the load in Figure 18. To draw all of the available power, the load should be around 5 GΩ.

2 | CONCLUSION

This paper presents an insight study for the zigzag triboelectric nanogenerator device. Analytical derivation has been derived for zigzag using the main characteristics of the device. Examining the analytical results, a well-established verified model is demonstrated using COMSOL simulation to verify them. The open circuit voltage, V_{OC} and short circuit charge, Q_{SC} are verified from the results of COMSOL simulation. The variation of open circuit voltage indicates a rise with increasing the angle between the tribo-pairs until it reaches a maximum value at $\approx 90^{\circ}$, then decreases again with increasing the angle. Clearly, the short circuit charge indicates a decrease with increasing the angle between the tribo-pairs. V_{OC} and Q_{SC} exhibit an average error of 0.02% and 0.33% respectively, between the analytical model and FEM results.

The accuracy of the proposed analytical model has been motivating for developing a Verilog-A model to examine the characteristics of the TENG device under different load conditions. A case of simple circuit with resistive load is examined. The impact of the angle between the two tribo-pairs on the I and V is depicted at different resistive loads. A peak power of 5.2 mW is observed at $R = 10^{10}$ Ω.

A case of simple capacitive load has been also investigated. I and V vs the angle have been examined under different capacitive loads. A peak in the energy stored in the capacitor is observed at 10^{-12} F for 28 μJ. The maximum power has been observed for different frequencies. The higher the frequency of operation, the higher the power obtained. The performance of the device has been investigated for different number of pairs and area variations. Increasing the number of pairs raises the output power significantly. The optimal power values are 12, 35 and 58 mW corresponding to 20, 90 and 200 GΩ. Moreover, the area variations study shows that increasing the device length is more important than the width. The output power graph shows the performance for different combination of physical dimensions. TENGs are not only able to charge energy storage devices, but also can drive electronic devices directly without a rectifier unit.[20] Future work on this model is to obtain DC characteristics of the output V and I. Zigzag model still also needs efficiency, figure of merits and different material investigations for quantifying the performance of the device.

NOMENCLATURE LIST

Parameter	Definition	SI Units
L	Plate length	m
w	Plate width	m
d_1, d_2	Thickness of the dielectrics	m
ϵ_{r1}, ϵ_{r2}	Relative dielectric constants	-
σ	Surface charge density	C/m^2
E	The electric field between the two plates	V/m
ϵ_0	The permittivity of the free space	F/m
Q	The transferred charge between the two plates	C
A	Area of the plate	m^2
C	Capacitance	F
R	Resistance	Ohm
P	Output power	Watt
E_c	The stored energy	Joule

ORCID

Hassan Mostafa https://orcid.org/0000-0003-0043-5007

REFERENCES

1. Niu S, Wang ZL. Theoreticalsystems of triboelectric nanogenerators. *NanoEnergy*. 2015:14:161-192.
2. Niu S.*Theory of Triboelectric Nanogenerators for Self Powered Systems*. *Georgia Tech Library*. Atlanta, United States: Georgia Institute of Technology PhD Theses. 2016. https://smartech.gatech.edu/bitstream/handle/1853/54954/NIU-DISSERTATION-2016.pdf.
3. Ahmed A, Hassan I, Ibn-Mohammed T, et al. Environmental life cycle assessment andtechnoeconomic analysis of triboelectric nanogenerators. *Energy Environ*. 2017;10:653-671.
4. Khalid S, Raouf I, Khan A, Kim N, Kim H. A review of human-powered energy harvesting for smart electronics: recent Progress and challenges. *Int J Precision Eng Manufact Green Technol*. 2019;6(3):821-851.
5. Bai P, Zhu G, Liu Y, et al. Cylindrical rotating Triboelectric Nanogenerator. *ACS Nano*. 2013;7(7):6361-6366.
6. Lee L. Dual mechanism for metal-polymer contact electrification. *J Electrostat*. 1994;32(1):1-29.
7. Maximous GS, Fatahalla AM, Seleym A, Ashour TA, Mostafa H. A new CAD tool for energy optimization of DiagonalMotionMode of attached electrode Triboelectric Nanogenerators. *IEEE International NEW Circuits and Systems Conference (NEWCAS)*. 2018;16:331-334.
8. Zi Y, Niu S, Wang J, Wen Z, Tang W, Wang ZL. Standards and figure-of-merits for quantifying the performance of triboelectricnanogenerators. *Nat Commun*. 2015;6:8376.
9. Zhang C, Chen J, Xuan W, et al. Conjunction of triboelectric nanogenerator with induction coils as wireless power sources and self-powered wireless sensors. *Nature Communications*. 2020;11(1). http://dx.doi.org/10.1038/s41467-019-13653-w.
10. Wang ZL, Jiang T, Xu L. Toward the blue energy dream by triboelectric nanogenerator networks. *Nano Energy*. 2017;39:9-23. http://dx.doi.org/10.1016/j.nanoen.2017.06.035.
11. Bai P, Zhu G, Lin ZH, et al. Integrated multilayered Triboelectric Nanogenerator for harvesting biomechanical energy from human motions. *ACS Nano*. 2013;7:3713-3719.
12. Zaky A, Ahmed A, Ibrahim P, Mahmoud B, Mostafa H. In-out cylindrical triboelectric nanogenerators based energy harvester. *61th IEEE International Midwest Symposium on Circuits and Systems (MWSCAS)*. 2018;61:1118–1121.
13. Wu C, Wang AC, Ding W, Guo H, Wang ZL. Triboelectric nanogenerator: a foundation of the energy for the new era. *Advanced Energy Materials*. 2019;9(1):1802906. http://dx.doi.org/10.1002/aenm.201802906.
14. Serway R, Jewett J, Peroomian V. Physics for scientists and engineers. *Boston: Cengage*. 2019;708-709.
15. Li A, Zi Y, Guo H, Wang ZL, Fernández FM. Triboelectric nanogenerators for sensitive nano-coulomb molecular mass spectrometry. *Nature Nanotechnology*. 2017;12(5):481-487. http://dx.doi.org/10.1038/nnano.2017.17.
16. Yang W, Chen J, Zhu G, et al. Harvesting energy from the natural vibration of human walking. *ACS Nano*. 2013;7:11317-11324.
17. Zaky A, Shehata M, Ismail Y, Mostafa H. Characterization and model validation of triboelectric nanogenerators using Verilog-a. *60th IEEE International Midwest Symposium on Circuits and Systems (MWSCAS)*. 2017;60:1536-1539.
18. Onsy E, El-Sttar R, Maximous G, Zaky A, Mostafa H. Complete study for diagonal Triboelectric Nanogenerators based energy harvester with computer aided design tool. *J Low Power Electron*. 2019;15(1):51-63.

19. Niu S, Liu Y, Zhou YS, Wang S, Lin L, Wang ZL. Optimization of triboelectric nanogenerator charging systems for efficient energy harvesting and storage. *IEEE Trans Electron Dev*. 2015; 62:641-642.
20. Liu D, Yin X, Guo H, et al. A constant current triboelectric nanogenerator arising from electrostatic breakdown. *Science Advances*. 2019;5(4):eaav6437. http://dx.doi.org/10.1126/sciadv.aav6437.

How to cite this article: Refaei A, Seleem M, Tharwat A, Mostafa H. A compact model for the zigzag triboelectric nanogenerator energy harvester. *Int J Energy Res*. 2021;45:1645–1660. https://doi.org/10.1002/er.5811